

Contents lists available at ScienceDirect

BBA - Bioenergetics

journal homepage: www.elsevier.com/locate/bbabio



Quantification of energy-converting protein complexes in plant thylakoid membranes

Vaclav Svoboda^a, Hui Min Olivia Oung^a, Haniyeh Koochak^a, Robert Yarbrough^a, Steven D. Mckenzie^b, Sujith Puthiyaveetil^b, Helmut Kirchhoff^{a,*}

ARTICLE INFO

Keywords: Quantitative biology Thylakoid membrane Photosystem II Photosystem I Cytochrome b₀f complex Light harvesting complex II

ABSTRACT

Knowledge about the exact abundance and ratio of photosynthetic protein complexes in thylakoid membranes is central to understanding structure-function relationships in energy conversion. Recent modeling approaches for studying light harvesting and electron transport reactions rely on quantitative information on the constituent complexes in thylakoid membranes. Over the last decades several quantitative methods have been established and refined, enabling precise stoichiometric information on the five main energy-converting building blocks in the thylakoid membrane: Light-harvesting complex II (LHCII), Photosystem II (PSII), Photosystem I (PSI), cytochrome $b_0 f$ complex (cyt $b_0 f$ complex), and ATPase. This paper summarizes a few quantitative spectroscopic and biochemical methods that are currently available for quantification of plant thylakoid protein complexes. Two new methods are presented for quantification of LHCII and the cyt $b_0 f$ complex, which agree well with established methods. In addition, recent improvements in mass spectrometry (MS) allow deeper compositional information on thylakoid membranes. The comparison between mass spectrometric and more classical protein quantification methods shows similar quantities of complexes, confirming the potential of thylakoid protein complex quantification by MS. The quantitative information on PSII, PSI, and LHCII reveal that about one third of LHCII must be associated with PSI for a balanced light energy absorption by the two photosystems.

1. Introduction

Quantitative biology has become a crucial research area in life sciences. This is manifested by the fact that dozens of research institutions around the world, scientific journals, and college majors have 'quantitative biology' in their names. The fast development of high-resolution imaging techniques combined with improvements in quantitative biochemical and biophysical techniques pave the way for a realistic description and modeling of biological systems like the virtual cell [1] or cell signaling networks [2]. Merging computational/simulation approaches with experimentally acquired quantitative data turns out to be a powerful tool for a mechanistic understanding of the functioning of the cell and its organelles at molecular resolution. Photosynthesis is a prime example where over the last decade computer modeling fed by experimentally-derived quantitative data was employed to describe the conversion of sunlight into chemical energy. Computational models and simulations ranging from coupled differential or steady state rate

equations [3–6] and coarse grain thylakoid models [7–9] to all-atomic molecular dynamics simulation (reviewed in [10]) have been used for describing energy conversion in isolated protein complexes, thylakoid membranes, and whole plant $\rm CO_2$ fixation and beyond. These models require precise information about the abundances and stoichiometric ratios of energy-converting protein complexes.

Thylakoid membranes host five main protein complexes that catalyze photosynthetic energy conversion: Photosystem (PS)II, PSI, light-harvesting complex (LHC)II, cytochrome b_6f (cyt b_6f) complex and the ATP synthase. All five are membrane-spanning integral protein complexes that are laterally non-randomly distributed between stacked grana thylakoids and unstacked stroma lamellae. PSII with LHCII are concentrated in stacked grana whereas PSI (with four LHCI) and ATPase are mainly found in unstacked thylakoid regions [11]. Fully active PSII is organized as dimeric supercomplex (C2S2M2), comprising a dimeric core (C2), two strongly-bound LHCII-trimers (S2), and two moderately-bound LHCII trimers (M2) [12,33,37]. Oligomeric states of LHCII

E-mail address: kirchhh@wsu.edu (H. Kirchhoff).

^a Institute of Biological Chemistry, Washington State University, Pullman, WA, USA

^b Department of Biochemistry and Center for Plant Biology, Purdue University, West Lafayette, IN 47907, USA

^{*} Corresponding author.

(trimer), cvt $b_6 f$ complex (dimer) [12] and very recently PSI (dimer [13]) have been described in plant thylakoids. After the discovery of the 'Z-scheme' of photosynthetic electron transport in the middle of the last century (reviewed in [14]), which describes the linear flow of electrons from the water splitting PSII to the NADP⁺-reducing PSI via the cyt b_6f complex, it was initially assumed that all energy-converting protein complexes occur at equal stoichiometries in plant thylakoid membranes. Later, however, multiple experimental evidence suggests that the ratios of PSII, PSI, LHCII, cyt $b_6 f$ complex, and ATPase are not equal but that their relative abundances are highly dynamic. For example, acclimation of photosynthetic organisms to changing environmental cues includes changes in relative protein complex stoichiometries in thylakoid membranes [15]. A well described phenomenon is photosystem stoichiometry adjustment wherein the relative abundance of the two photosystems changes in order to maximize light energy conversion under varying light quality conditions [16-18]. A sunlight intensityinduced alteration in the abundance of PSII, LHCII, cyt b_6f complex and ATPase has also been noted [15,19]. For tracking these compositional acclimation responses and for serving the upcoming need of computational approaches to describe energy conversion, solid experimental methods are required that quantify the main energy-converting building blocks of the thylakoid membrane. In this paper we summarize, in our view, some of the quantitative methods for determining the abundance of LHCII, PSII, cyt b₆f complex, PSI, and ATPase. New approaches are presented for quantifications of LHCII and cyt $b_6 f$ complex.

2. Methods

2.1. Thylakoid membrane isolation

Thylakoid membranes were harvested from 6 to 7 weeks old Arabidopsis thaliana Col-0 plants grown under 9 h of illumination a day at a light intensity of 120 μ mol/m²/s. Leaves from two fully grown rosettes were harvested in cold room and immediately homogenized in 50 mL of ice cold grinding buffer (20 mM Tricine (pH 8.4), 400 mM Sorbitol, 10 mM EDTA, 10 mM NaHCO₃, 10 mM NaF, and 0.15 % BSA) using a Waring blender. The homogenate was filtered through a sandwich of a small Kimwipe, 4 layers of cheesecloth, and a layer of miracloth, and the filtrate was divided into two equal volumes in ice cold glass tubes and spun at 2000 $\times g$ for 2 min using a swing bucket rotor. The supernatant was discarded, and the pellet resuspended in 5-10 mL of shock buffer (25 mM HEPES (pH 7.5), 40 mM KCl, 7 mM MgCl₂, 10 mM NaF, and 0.4 mM Pefabloc) using a fine brush until no coarse particles were visible. The final volume was adjusted to 40 mL and incubated on ice for 10 min in dark. Thylakoids were spun down in a fixed angle rotor at 4000 $\times g$ for 10 min. The supernatant was discarded, and the pellet resuspended in 700 µL of storage buffer (50 mM HEPES (pH 7.5), 100 mM Sorbitol, 5 mM MgCl₂, 10 mM NaF, 0.4 mM Pefabloc, and PhosSTOP (Roche, 1 tablet per 10 mL buffer)) using a fine brush. 300 µL of additional storage buffer was used to retrieve residual thylakoids from the brush. The thylakoid suspension was transferred to a 1.5 mL Eppendorf tube and washed once in storage buffer by repeating the centrifugation (1500 $\times g$ for 10 min) and resuspension steps. Total volume of thylakoid suspension was kept at ~ 1.0 mL. Protease and phosphatase inhibitors were always added fresh before isolation and all centrifugation steps were done at 4 °C.

Chlorophyll determination was done according to Porra et al. [22] using a Hitachi U3900 spectrometer. Absorption was measured at 646.6 nm, 663.6 nm, and 750 nm. For chlorophyll extraction, 3 μL thylakoid suspension was added to 1 mL 80 % Acetone solution, thoroughly vortexed, and spun down at 18000 $\times g$ for 10 min. 500 μL of the resulting supernatant was used for absorption measurement.

2.2. Difference absorption spectroscopy

2.2.1. Cytochromes

Quantification of cytochromes b_6 , f, and b_{559} was done by difference absorption spectroscopy. For the measurement, thylakoids were resuspended in Difference Absorption Spectroscopy (DAS) buffer (330 mM sorbitol, 20 mM HEPES (pH 7.6), 10 mM KCl, 50 μM EDTA and 0.18 %(w/v) β -dodecylmaltoside) and the absorption at a spectral range of 540 to 575 nm was recorded with a Hitachi U3900 spectrometer (2-nm slit width). The DAS buffer was pre-warmed to room temperature to minimize spectroscopic jitter. Chlorophyll concentration in the cuvette was adjusted to 25 to 40 μM as determined by the maximum peak at 677.5 nm (spectral range: 600-750 nm). Cytochromes were quantified as described in Kirchhoff et al. [20] with minor modifications. The redox change was induced by incubating samples consecutively with 1 mM potassium ferricyanide for 1 min, 4 mM sodium ascorbate for 5 min, and 5 mM sodium dithionite for 5 min. A layer of paraffin oil was added on top of the samples after dithionite treatment to avoid reaction with air and the subsequent formation of dithionite decomposition products. A liquid form of dithionite was used for preventing artifacts produced by excess dithionite and for increasing the reproducibility of the results.

2.2.2. P700

Isolated thylakoid membranes were diluted in a buffer containing 330 mM sorbitol, 20 mM HEPES (pH 7.6), 10 mM KCl, 50 μ M EDTA and 0.03% (w/v) β -dodecylmaltoside at a chlorophyll concentration of 30 μM. Oxidized minus reduced P700 redox changes was measured at 705 nm with a homebuilt flash spectrometer. 100 µM methyl viologen was added as an electron acceptor for P700 and 5 mM sodium ascorbate, as an electron donor. A quantitative redox change was triggered by a 200 ms long saturating light pulse (>3000 μ mol photons m⁻² s⁻). Measurements were repeated 4 to 9 times and averaged. A drift signal and a light pulse artefact signal were recorded by repeating the measurements but without the light pulse or without measuring light and then subtracted them from the signal with the light pulse. Data were analyzed with SigmaPlot 11 software. The maximal light-induced absorption change was converted into mM P700 by using a difference extinction coefficient of 64 mM⁻¹ cm⁻¹ [21]. After the measurement, the exact Chl concentration in the cuvette was measured spectroscopically using an acetonic extract of the samples according to [22].

2.3. Cytochrome heme staining

Heme specific staining was done according to Fristedt et al. [23] with some modifications. Samples were solubilized on ice for 40 min in dark with 100 mM dithiothreitol (DTT) in a sample buffer (40 mM Tris, 8 % Glycerol, 2.5 % SDS, and 0.01 % Bromphenol blue). Incubation on ice is important as room temperature affects heme signal intensity (not shown). Thylakoid proteins were first separated by SDS-PAGE using a 5 % stacking and a 10 % separating gel [24]. TMBZ (3,3',5,5'-Tetramethylbenzidine) staining was done essentially as in Fristedt et al. [23]. TMBZ was first dissolved in methanol in dark. 1 M sodium acetate (NaOAc pH 5) was added to obtain a final concentration of 0.25 M NaOAc and 6.3 mM TMBZ. The gel was placed in the staining solution, covered, wrapped in aluminum foil, and agitated in a dark box on ice for 45 min for a homogenous incubation. The gel was subsequently incubated in a 30 mM hydrogen peroxide solution until bands were visible and then the peroxide solution was replaced with water. After heme staining and documentation, the gel was subsequently stained with Coomassie brilliant blue (CBB) to generate corresponding controls. Commercially available cytochrome c (12 kDa) from equine heart was used as standard for heme quantification (CAS 9007-43-6, Sigma-Aldrich). We observed that concentration of DTT is critical for full development of cytochrome c heme signal. Concentrations of DTT lower than 75 mM showed lower staining intensity (not shown).

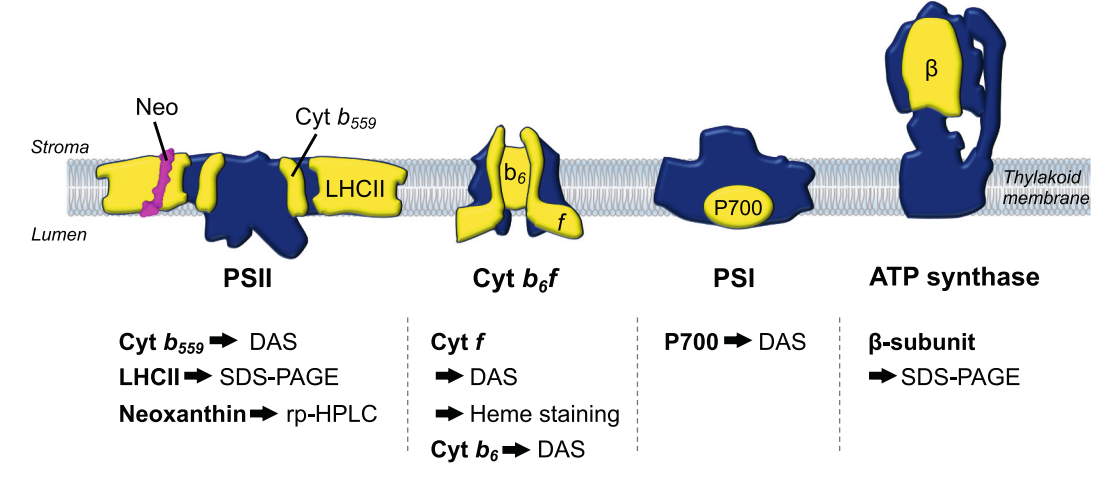


Fig. 1. An overview of the main protein supercomplexes in plant thylakoid membranes. Protein subunits and chromophores used for the quantification of supercomplexes are highlighted in yellow with the carotenoid neoxanthin (Neo) in purple. The bottom panel summarizes the methods that have been employed for the quantifications. DAS, difference absorption spectroscopy; rp-HPLC, reverse-phase high performance liquid chromatography.

2.4. Quantitative SDS PAGE gel electrophoresis

2.4.1. ATPase

The ATPase protein content was determined by densitometric analysis of the protein band of ATPase β -subunit on a Coomassie-stained SDS-PAGE gel (16 % Tris-Glycine). In order to quantify the protein, a dilution series of the isolated ATPase protein standards were run on the same gel with the sample (see Fig. 7). Using the Image-Pro Plus software, the staining intensity of the sample was compared with the staining intensity of the isolated protein standard. The results of the band analysis were then presented as mmol ATPase/mol Chl [25].

2.4.2. LHCII

The LHCII content in thylakoid membranes was determined using comparative densitometric analysis of protein band intensity using isolated LHCII as protein standard. LHCII from spinach was isolated according to [26]. Thylakoid samples were first resolved along with known amount of LHCII protein standard on a 5 % stacking and 12 % separating gel containing 6 M urea according to Laemmli [27]. Samples were first solubilized at 50 °C for 30 min in a sample buffer containing 2 % β -mercaptoethanol and spun down before loading. Coomassie staining of the protein gel was done overnight at room temperature with gentle agitation in a solution containing 50 % methanol, 10 % glacial acetic acid, and 0.25 % (w/v) CBB. Destaining was done in the same solution without CBB until no background was visible. The staining intensity was analyzed as before using the Image-Pro Plus software and the LHCII content was expressed as mmol/mol Chl.

2.5. Reversed phase (rp) HPLC

Isolated thylakoid samples equivalent to 1 μg chlorophyll were mixed with 125 μL of 87 % acetone containing 0.1 mM Tris and centrifuged for 2 min at 25,000 $\times g$. The supernatant was transferred to a new microcentrifuge tube and the pellet was resuspended in 150 μL of 100 % acetone for complete pigment extraction. The resuspended pellet was further centrifuged for 2 min at 25,000 $\times g$. The supernatants from these two centrifugation steps were then pooled and filtered using a 0.20 μm filter. The filtrate (pigment extract) was then analyzed using a reversed-phase high-performance liquid chromatography (RP-HPLC) (Shimadzu) equipped with a LiChrosorb RP-18 (5 μm) column, as described in Färber et al. [28]. The column temperature was set at 35 °C for a better separation of peaks. The mobile phase consists of solvent A (acetonitrile:methanol:Tris buffer (0.1 M pH 8.0) at a ratio of 87:10:3) and solvent B (methanol:n-Hexane at a ratio of 4:1). The gradient from

solvent A to B starts at 9 to 12.5 min (flow rate 2 mL/min). Eluted neoxanthin was monitored at 440 nm and chlorophyll a (Chl a) and b (Chl b), at 660 nm. The area under the retention profile was calibrated to pmol pigment with pure pigment standards: 2.8000×10^{-4} area per pmol for neoxanthin, 5.2985×10^{-4} area per pmol for Chl a, and 6.2580×10^{-4} area per pmol for Chl b. The amount of LHCII was calculated by the equation.

 $LHCII_3/Chl = (neoxanthin/Chl - 2 \times PSII/Chl)/3$

2.6. Label-free quantitative mass spectrometry

The relative abundance of PSII, PSI, cytochrome b_6f complex, and ATPase has been quantified using label-free mass spectrometry. Thylakoid membranes from Arabidopsis plants grown under short-day (8 h light/16 h dark) white light condition (\sim 150 µmol photons m⁻² s⁻¹) were isolated as described earlier. Thylakoid proteins were extracted from the membrane by incubation in an extraction buffer (4 % sodium dodecyl sulfate (SDS), 40 mM dithiothreitol (DTT), and 40 mM Tris-HCl (pH 8.0)) at 80 $^{\circ}$ C for 10 min. The extracted proteins were precipitated from the reaction mixture using a chloroform-methanol solution in a 1:4 chloroform:MeOH ratio, followed by centrifugation at 18,800 ×g in a microcentrifuge at room temperature for 10 min. The precipitated pellet was washed with additional methanol before pellets were dried and resuspended in 8 M Urea, 20 mM Tris-HCl (pH 8.0) and 3 mM EDTA and the protein concentration was measured by BCA assay (Pierce). Cysteine residues in protein samples were reduced by dithiothreitol and alkylated by iodoacetamide before digestion with 4 µg Trypsin/Lys-C (Promega) prepared in 50 mM ammonium bicarbonate at 37 °C for 16 h as described in McKenzie et al. [29]. The digested peptides were desalted using a C18 spin column (The Nest Group) and resuspended in 3 % acetonitrile and 0.1 % formic acid. Peptides equivalent to one microgram were analyzed by reverse-phase LC-ESI-MS/MS using the Dionex UltiMate 3000 RSLC nano System coupled to the Q Exactive High Field (HF) Orbitrap Mass Spectrometer (Thermo Fisher Scientific) as described earlier [29].

Mass spectra were searched against The *Arabidopsis* Information Resource (TAIR) proteome database (v.10). For label-free quantification, a normalized measure of molar abundance of individual proteins known as the relative intensity-based absolute quantification (riBAQ) was used [30]. It is calculated by dividing each protein's iBAQ value by the sum of all unfiltered iBAQ values in the corresponding sample. The abundance of each thylakoid protein complex is the mean riBAQ value of a set of constituent subunits that are common to all biological

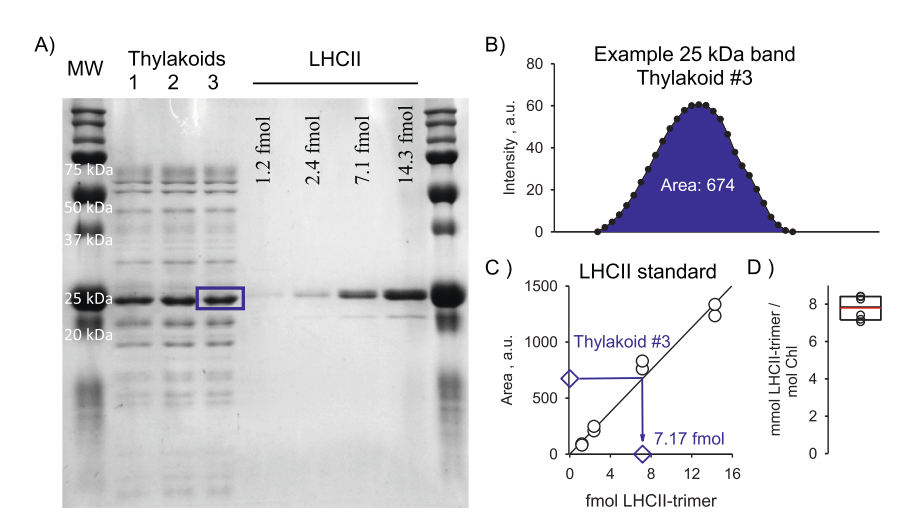


Fig. 2. LHCII quantification by quantitative SDS PAGE. 2A, Example of a gel with three thylakoid membrane samples (1 to 3, left) and four different amounts of isolated LHCII standards. The fmol numbers give the amount of trimeric LHCII put on each lane. Blue rectangle indicates the LHCII 25 kDa band whose intensity was profiled as an example in 2B. MW, molecular weight standard. 2B, Intensity profile of the LHCII band from lane #3 with the corresponding area under the curve. 2C, LHCII calibration curve generated from isolated LHCII standard (right lanes in panel A). As an example, the conversion of the area deduced in panel B into fmol of trimeric LHCII is shown for the thylakoid sample #3. D, Statistical distribution of LHCII quantification data points for thylakoid membranes. Red lines indicate the mean value.

replicates as listed in [17]. The abundance of PSII and PSI was calculated from the values of reaction center core subunits to account for the differing antenna composition and antenna size.

3. Results and discussion

The quantification of protein complexes in thylakoid membranes requires a reference point to which the amounts could be expressed as relative values. Potential reference parameters can be thylakoid membrane area, total thylakoid lipids, total thylakoid protein, or a reference protein complex. However, a straightforward measure for the amount of the thylakoid membrane is the chlorophyll content. Since chlorophylls are exclusively localized in thylakoid membranes and their content relates directly with the most abundant Chl-binding protein complexes (LHCII, LHCI, PSI, and PSII), they can be a good proxy for the membrane [20]. Furthermore, the chlorophyll content can easily be quantified by spectrophotometric measurements of organic solvent extracts [22]. Therefore, the following protein complexes will be quantified on a molar basis relative to total chlorophyll. Our approaches for quantification of thylakoid protein complexes and supercomplexes involve measuring the

amount of a marker chromophore or a protein subunit within each complex that has a well-defined stoichiometric ratio to that complex. Fig. 1 gives an overview of these protein complex markers (in bold) that were employed in this study together with the methods that quantify them. This approach was made possible by the excellent high-resolution protein structural data that are now available for plant thylakoid membranes.

3.1. Quantification of LHCII

The LHCII protein family in higher plants can be divided into the major trimeric LHCII (made of Lhcb1, Lhcb2, and Lhcb3 subunits) and the minor monomeric CP29 (Lhcb4), CP26 (Lhcb5), and CP24 (Lhcb6) [31,32]. The minor LHCIIs are tightly bound to the PSII core with a 1:1 stoichiometry of each minor LHCII subunit to PSII monomer [32]. Furthermore, in *Arabidopsis* a population of the major trimeric LHCII associates with the dimeric PSII core via the three minor antennae proteins, forming the C2S2M2 supercomplex [33] with a trimeric LHCII to PSII-monomer ratio of two to one. However, native thylakoid membranes contain a variable amount of additional 'loosely'-bound or 'free'

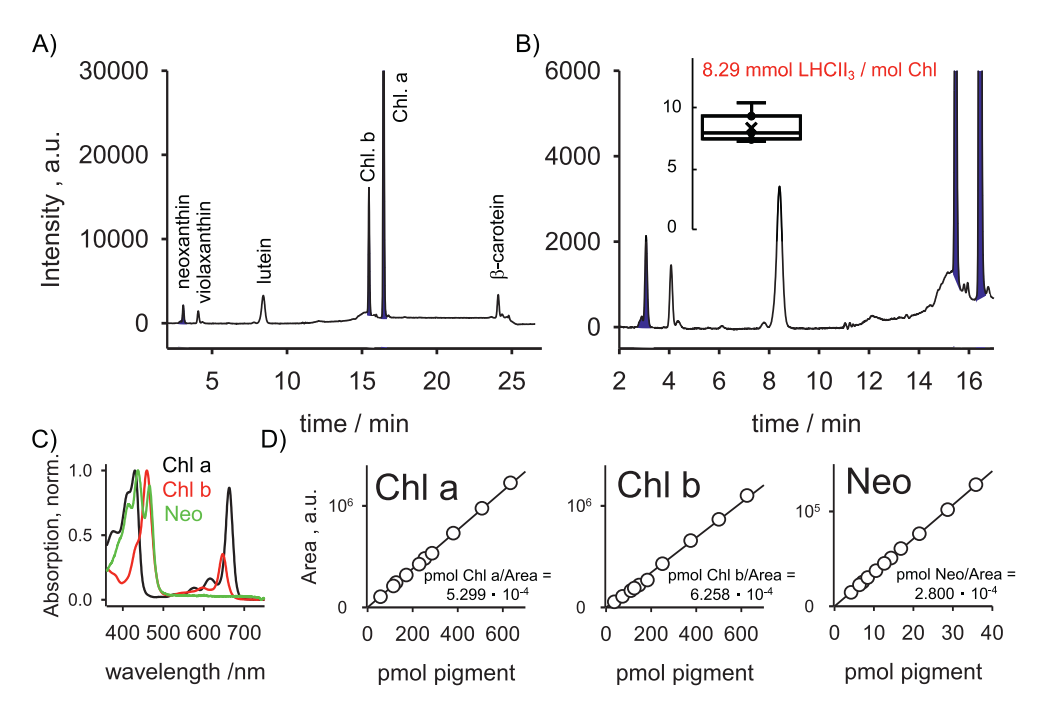


Fig. 3. LHCII quantification by rp-HPLC method. A, Example of an rp-HPLC chromatogram. The separated pigments are indicated. Detection wavelength, 440 nm; spectral bandwidth, 8 nm. B, zoomed-in view highlighting the areas (in blue) for neocanthin (retention time ~3.2 min), Chl b (retention time ~15.5 min), and Chl a (retention time ~16.5 min). C, Normalized absorption spectra of isolated pigments in ethanol used to generate calibration curves. D. Calibration curves at 440 nm for Chl a. Chl b, and Neo used to convert the areas under the pigment peaks (see B) to pmol pigments. The conversion factors are given for each pigment. The statistical analysis for LHCII quantification by rp-HPLC is given as an inset in panel B.

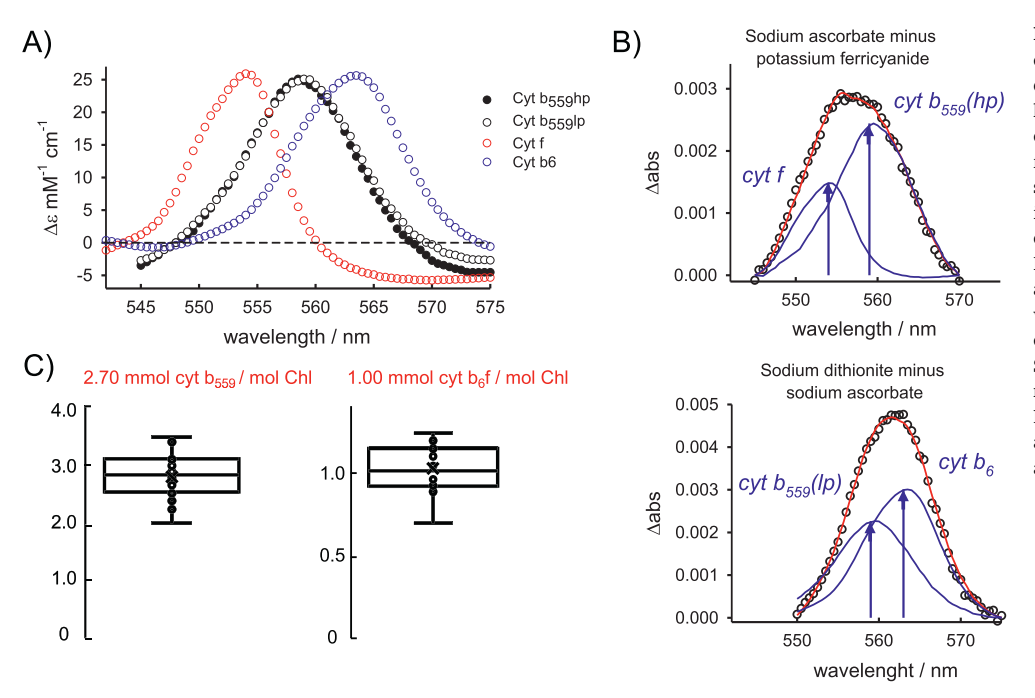


Fig. 4. Quantification of thylakoid cytochromes by DAS. A, Reference spectra with differential extinction coefficients ($\Delta \epsilon$) for hemes of the two cyt b_{559} forms, cyt b_6 , and cyt f. B, Examples of chemical induced DAS for a thylakoid sample. The cytochromes showing up at different redox treatments are indicated in blue. Red lines give the fitted curves that are sums of the blue curves. Black circles represent measured data points and the blue arrows indicate the amplitude values (in Δ abs units), which were used to calculate the cytochrome concentrations, C. Statistics of cyt quantifications of thylakoid membranes. For the quantification of total PSII, cyt b_{559} (hp) and cyt b_{559} (lp) were added, and for quantification of cyt $b_6 f$, the average of cyt f and cyt $b_6/2$ was used.

trimeric LHCII. The amount of total LHCII (bound within C2S2M2 plus 'loosely'-bound LHCII) per PSII reaction center depends on light conditions (e.g. [19]). Published ratios of total LHCII-trimers per PSII-monomer range from 4 under high light to over 7 in low light-acclimated plants [19,34,35]. The higher ratio in low light is the result of plants increasing their capacity for harvesting the limiting solar radiation. For LHCII, no specific redox-dependent difference absorption spectra exist. Therefore, employing difference absorption spectroscopy for LHCII quantification, as used for PSII, PSI, and cyt $b_0 f$ complexes, is not possible. Two alternative approaches based on gel electrophoresis and HPLC are introduced below.

3.1.1. SDS-PAGE gel quantification of the major LHCII complex

A technique to quantify trimeric LHCII in thylakoid membranes using gel electrophoresis is shown in Fig. 2 [20]. This method is based on comparing the Coomassie staining intensity of the 25 kDa LHCII band in thylakoid samples with that of isolated LHCII protein, which is used as standard and run on the same denaturating SDS-PAGE gel (Fig. 2A). Under our gel running conditions the 25 kDa band contains the Lhcb1, Lhcb2, and Lhcb3 isoforms that make up the trimeric LHCII. The minor CP26 and CP29 proteins run higher on an SDS-PAGE gel whereas CP24 as well as the LHCI subunits run below the 25 kDa band [36-38] as expected from their theoretical molecular weight [31]. Thus, the protein band around 25 kDa mass is ideal for trimeric LHCII quantification as it is devoid of other protein subunits. The isolated LHCII standard has a small contamination from CP24 [36,37], seen as a faint band below the dominant 25 kDa band. However, the intensity of this band is negligible (~5 % CP24 band intensity relative to 25 kDa band intensity). An important prerequisite for protein quantification by an SDS PAGE gel is the linearity of the (Coomassie) stain signal over a certain range of protein amount. Fig. 2C demonstrates that this linearity is obtained for the range of LHCII standard loaded on the gel covering an order of magnitude. Note that the staining intensity of the 25 kDa band of the unknown thylakoid sample is within the range of the LHCII standard regression curve (Fig. 2C), ensuring its proper quantification. From the calibration curve in Fig. 2C, the fmol LHCII in the thylakoid samples is deduced and set in relation to the Chl content of this sample. For example, from the 7.17 fmol of LHCII for the thylakoid sample #3 (Fig. 2C) and the 1 pmol of Chl put on the gel a LHCII to Chl ratio of 7.17

mmol/mol Chl is given. This method gives a mean value of 7.8 mmol LHCII trimer per mol of Chl (Fig. 2D).

3.1.2. Major LHCII quantification by reversed phase (rp)HPLC

Fig. 3 presents a new method for the quantification of the major LHCII protein complex in thylakoid membranes. This approach makes use of the observation that the xanthophyll neoxanthin (neo) is exclusively found in LHCII proteins [33,39]. Moreover, high-resolution PSII structures reveal that each trimeric LHCII contains three non-covalently but tightly bound neoxanthins (one per monomer). The monomeric CP29 and CP26 each contain one neoxanthin as well [33]. Thus, neo serves as an excellent marker pigment for LHCII quantification. The quantification of thylakoid pigments from organic extracts of thylakoid membranes by reversed phase HPLC at 440 nm detection wavelength (Fig. 3A) is a well-established method [28,40]. The areas under the peaks in Fig. 3A (Fig. 3B is a zoomed-in image) are directly proportional to pmol pigments. For the conversion of area to pmol pigments, calibration curves with isolated pigments were conducted. The purity of the pigments was verified by HPLC runs and their concentration quantified by absorption spectroscopic measurements (Fig. 3C). The calibration curves in Fig. 3D reveal good linearity for Chl a, Chl b, and neo for the given pmol range. The conversion factors for the three pigments (given in Fig. 3D) agree with literature values [28]. Slight differences are expected since HPLC settings like optical bandwidth can lead to small deviations. Since the PSII-bound CP26 and CP29 each contain one neo the measured neo values were corrected by subtracting 2-times the amount of PSII (for PSII quantification see below). In case that the PSII amount cannot be determined the uncorrected neo content is still a good estimate for the major LHCII content. For example, the amount of LHCII for our Arabidopsis thylakoids would change from 0.61 pmol LHCII (without correction for the CP26 and CP29 contribution) to 0.49 pmol LHCII (with correction), i.e. the error for the uncorrected values is a \sim 20 % overestimation. The final LHCII-trimer to Chl ratio is calculated by dividing the corrected neo values by the Chl content (in mol) and by three (three neoxanthins per trimer) giving a LHCII trimer to Chl ratio of 8.3 (inset Fig. 3B). The advantages of rp-HPLC-based LHCII quantification is that this method is more quantitative than SDS PAGE-based quantification and that it can be applied to organic leaf extracts. Regardless, both methods give a consistent LHCII-trimer quantification

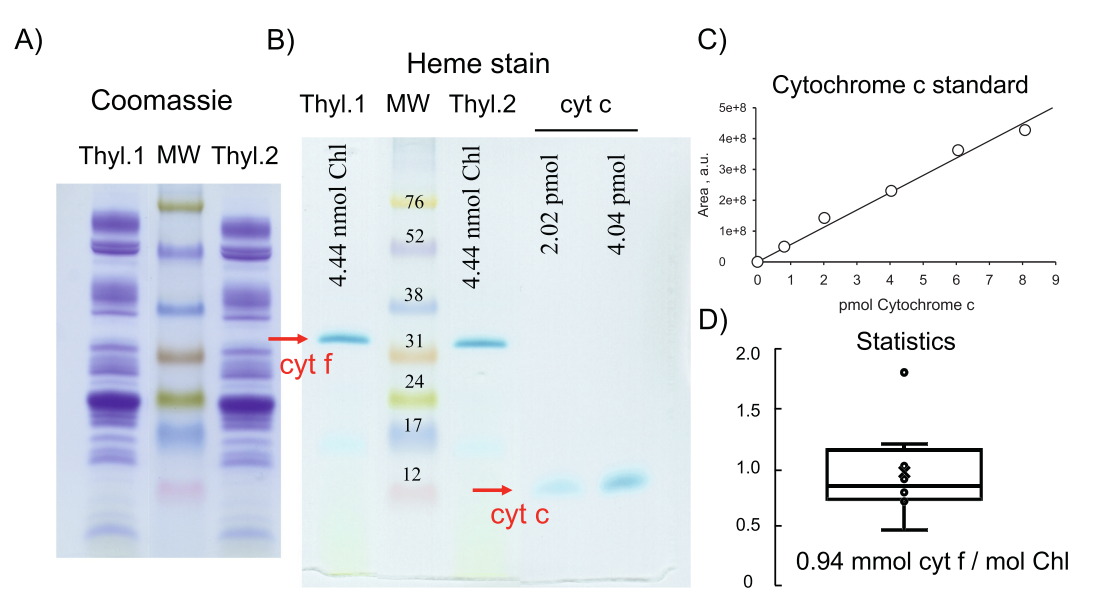


Fig. 5. Quantification of cyt f in thylakoid samples by heme staining. A, Example of a Coomassie stained SDS PAGE showing two thylakoid samples (4.44 nmol Chl per lane) with molecular weight standard (MW). B, TMBZ staining of the same gel (also containing cyt c standards that are not shown in A). The positions of cyt f and cyt c are indicated (red). Quantifications of band intensities was done as with LHCII gels (see Fig. 2) C, A plot of the band intensity area versus the amount of the cyt c standard demonstrating that the sample concentrations were in the linear range. D, Statistics of cyt f quantification by heme staining.

of about 8 mmol LHCII per mol of Chl.

3.2. Quantification of PSII and cyt b₆f complex

3.2.1. Difference extinction coefficients of cytochrome α -bands

A wide range of extinction coefficients ranging from 15 to 23.4 $\mathrm{mM}^{-1}\,\mathrm{cm}^{-1}$ for the α -band of reduced minus oxidized cyt b_{559} has been reported [41]. This holds also for the cytochromes of the cyt $b_6 f$ complex [42]. Before applying difference absorption spectroscopy for quantification of cytochromes in thylakoid membranes, the exact extinction coefficients have to be determined. Arguing for a higher value, a critical analysis of the cyt f reduced minus oxidized difference extinction coefficients by [42] provides plausible reasons for the discrepancy found in the literature. For reevaluation of the cyt b_{559} extinction coefficient, we used a PSII preparation isolated from the cyanobacterium Synechococcus elongatus, (kind gift from Dr. Mathias Rögner, University of Bochum, Germany). From HPLC-based quantifications of phaeophytin and chlorophylls at 660 nm, a Chl/PSII monomer ratio of 39 was determined for this preparation (not shown). The midpoint redox potential of the high potential (HP) cyt b_{559} (370–435 mV) [43] allows its complete oxidization and reduction by potassium ferricyanide and sodium ascorbate, respectively. Further addition of sodium dithionite induces a quantitative redox change in oxidized/reduced low potential (LP) form of cyt b_{559} since its redox midpoint potential is 0-80 mV [43]. The corresponding reduced minus oxidized difference absorption spectra of cyt b_{559} (HP) and cyt b_{559} (LP) of the PSII preparation are shown in Fig. 4A. Although these absorption difference spectra were recorded from a cyanobacterium the shapes of the absorption spectra are very similar to the ones reported for higher plants [43], i.e. the absorption maximum is at 559 nm and the full width at half maximum is 10.0 nm. The extinction coefficients for the cyt b_{559} difference absorption spectra were determined from the maximum difference absorption signal at 559 nm minus the isosbestic point at 548 nm, the Chl concentration in the spectrometer cuvette, and the Chl/PSII monomer core ratio of 39, leading to a coefficient of 25.1 mM⁻¹ cm⁻¹ for both the high and low potential forms (Fig. 4A).

The difference absorption coefficients for the α -bands of cyt f and cyt b_6 were derived from isolated dimeric cyt $b_6 f$ complex from tobacco plants. The reduced minus oxidized difference spectrum of cyt f (sodium

ascorbate minus potassium ferricyanide), peaking at 554 nm (Fig. 4A), is identical to published spectra [42,44]. The extinction coefficient for cyt f at 554 nm, corrected for the isosbestic point at 554.3 nm, was set to 25.2 mM⁻¹ cm⁻¹ [42]. The amplitude of the reduced minus oxidized difference absorption spectrum of cyt b_6 (corrected for the isosbestic point at 543 nm, [44]) in our cyt $b_6 f$ complex preparation is twice as high as for cyt f (exact number 2.02). Our approach to determine the extinction coefficient of cyt b_6 is to assume a molar cyt b_6 to cyt f ratio of two since this is the settled stoichiometry of hemes revealed by the high-resolution structures of this complex [45,46]. It thus follows that the reduced minus oxidized difference extinction coefficient for cyt b_6 at 563 nm is $25.5 \text{ mM}^{-1} \text{ cm}^{-1} (2.02 / 2 [b_6 \text{ per } b_6 f \text{ complex}] * 25.2 \text{ mM}^{-1} \text{ cm}^{-1} [\text{for } b_6 f \text{ complex}] * 25.2 \text{ mM}^{-1} \text{ cm}^{-1} [\text{for } b_6 f \text{ complex}] * 25.2 \text{ mM}^{-1} \text{ cm}^{-1} [\text{for } b_6 f \text{ complex}] * 25.2 \text{ mM}^{-1} \text{ cm}^{-1} [\text{for } b_6 f \text{ complex}] * 25.2 \text{ mM}^{-1} \text{ cm}^{-1} [\text{for } b_6 f \text{ complex}] * 25.2 \text{ mM}^{-1} \text{ cm}^{-1} [\text{for } b_6 f \text{ complex}] * 25.2 \text{ mM}^{-1} \text{ cm}^{-1} [\text{for } b_6 f \text{ complex}] * 25.2 \text{ mM}^{-1} \text{ cm}^{-1} [\text{for } b_6 f \text{ complex}] * 25.2 \text{ mM}^{-1} \text{ cm}^{-1} [\text{for } b_6 f \text{ complex}] * 25.2 \text{ mM}^{-1} \text{ cm}^{-1} [\text{for } b_6 f \text{ complex}] * 25.2 \text{ mM}^{-1} \text{ cm}^{-1} [\text{for } b_6 f \text{ complex}] * 25.2 \text{ mM}^{-1} \text{ cm}^{-1} [\text{for } b_6 f \text{ complex}] * 25.2 \text{ mM}^{-1} \text{ cm}^{-1} [\text{for } b_6 f \text{ complex}] * 25.2 \text{ mM}^{-1} \text{ cm}^{-1} [\text{for } b_6 f \text{ complex}] * 25.2 \text{ mM}^{-1} \text{ cm}^{-1} [\text{for } b_6 f \text{ complex}] * 25.2 \text{ mM}^{-1} \text{ cm}^{-1} [\text{for } b_6 f \text{ complex}] * 25.2 \text{ mM}^{-1} \text{ cm}^{-1} [\text{for } b_6 f \text{ complex}] * 25.2 \text{ mM}^{-1} \text{ cm}^{-1} [\text{for } b_6 f \text{ complex}] * 25.2 \text{ mM}^{-1} \text{ cm}^{-1} [\text{for } b_6 f \text{ complex}] * 25.2 \text{ cm}^{-1} [\text{for } b_6 f \text{ complex}] * 25.2 \text{ cm}^{-1} [\text{for } b_6 f \text{ complex}] * 25.2 \text{ cm}^{-1} [\text{for } b_6 f \text{ complex}] * 25.2 \text{ cm}^{-1} [\text{for } b_6 f \text{ complex}] * 25.2 \text{ cm}^{-1} [\text{for } b_6 f \text{ complex}] * 25.2 \text{ cm}^{-1} [\text{for } b_6 f \text{ complex}] * 25.2 \text{ cm}^{-1} [\text{for } b_6 f \text{ complex}] * 25.2 \text{ cm}^{-1} [\text{for } b_6 f \text{ complex}] * 25.2 \text{ cm}^{-1} [\text{for } b_6 f \text{ complex}] * 25.2 \text{ cm}^{-1} [\text{for } b_6 f \text{ complex}] * 25.2 \text{ cm}^{-1} [\text{for } b_6 f \text{ complex}] * 25.2 \text{ cm}^{-1} [\text{for } b_6 f \text{ complex}] * 25.2 \text{ cm}^{-1} [\text{for } b_6 f \text{ complex}] * 25.2 \text{ cm}^{-1} [\text{for } b_6 f \text{ complex}] * 25.2 \text{ cm}^{-1} [\text{for } b_6 f \text{ complex}] * 25.2 \text{ cm}^{-1} [\text{for } b_6 f \text{ complex}] * 25.2 \text{ cm}^{-1} [\text{for } b_6 f \text{ complex}] * 25.2 \text{ cm}^{-1} [\text{for } b_6 f \text{ complex}] * 25.$ $\operatorname{cyt} f$]). The re-evaluation of the difference absorption coefficients in the α -band region reveals very similar numbers for all four cytochromes $(\sim 25 \text{ mM}^{-1} \text{ cm}^{-1})$ as speculated earlier [42]. The reference spectra shown in Fig. 4A pave way for quantification of cytochromes from difference absorption spectroscopy.

3.2.2. Quantification of PSII and cyt b_6 f complex by difference absorption spectroscopy

In the literature PSII has been quantified by different methods like estimation of atrazine-binding sites [47], EPR of tyrosine D [48,49], and reduced-minus-oxidized difference absorption spectroscopy of different redox active PSII centers like the so-called C550 signal (related to pheophytin) [20,50], the primary quinone acceptor Q_A (at 320 nm) [51], and cyt b_{559} [20,48]. Our choice to quantify PSII by cyt b_{559} difference absorption spectroscopy is based on the facts that (i) spectroscopy is highly quantitative, (ii) cyt b_{559} is an excellent marker for all PSII complexes since it has a fixed 1:1 stoichiometry per reaction center, and (iii) it is found in all structural forms of PSII ranging from the C2S2M2 holocomplex to truncated PSII monomers [33,52], and (iv) it is technically not costly, i.e. it requires only an absorption spectrometer. The same advantages are also apparent for using cyt f and cyt b_6 difference absorption spectroscopy for quantification of the cyt $b_6 f$ complex.

Fig. 4B presents examples of chemically induced difference absorption spectra measured on intact thylakoid membranes in the cytochrome α -band region. The upper panel shows difference spectra for sodium ascorbate (reduced) minus potassium ferricyanide (oxidized). Under these conditions only cyt f and cyt $b_{559}(\text{HP})$ signals appear. The lower

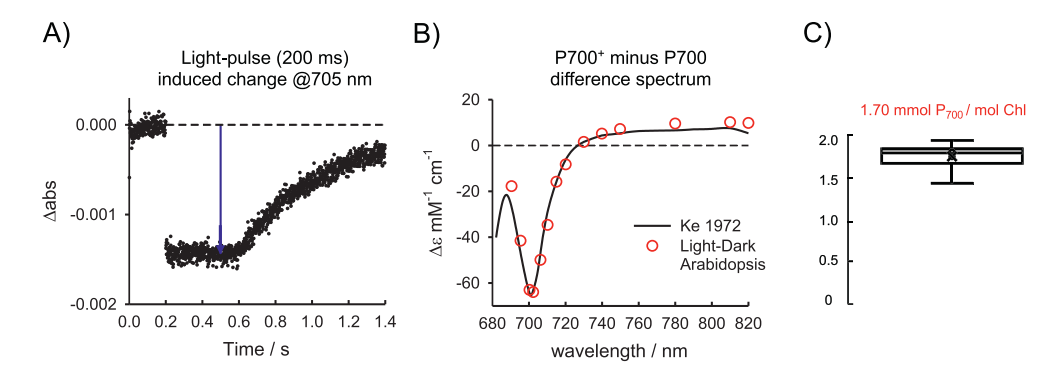


Fig. 6. Quantification of P700 by DAS. A, Example of a light induced absorption change (Δ abs) at 705 nm reflecting a P700 to P700⁺ redox change. The blue arrow indicates the maximal Δ abs used for P700 quantification. B, Comparison of (Δ abs) signals from isolated PSI preparation [21] and the light-induced Δ abs (example in A) from Arabidopsis thylakoid membranes. C, Statistics of P700 quantification by DAS.

panel gives the spectra of sodium dithionite (reduced) minus sodium ascorbate (oxidized) with contributions from cyt $b_{559}(LP)$ and cyt b_6 . To eliminate spectral contributions of non-cytochromes, redox active chromophores (e.g. P700 or PC), the spectral range was set narrowly around the peaks of the cytochromes (545 to 570 nm for cyt f and cyt $b_{559}(HP)$, 550 to 575 nm for cyt b_6 and cyt $b_{559}(LP)$). Furthermore, baselines were subtracted for these spectral regions to remove flat spectral contributions of redox active chromophores. The corrected difference absorption spectra displayed in Fig. 4B are highly enriched in cytochromes. For the separation of the two cytochromes in both difference spectra, a mathematical fitting procedure has been applied by using the baseline-corrected reference spectra in Fig. 4A with their amplitudes as the only free fitting parameters. For both conditions, the fitted spectra (red lines) described the measured data (black circles) well. The high quality of the mathematical fitting indicates the depletion of non-cytochrome chromophores. The contributions of the individual cytochromes are shown in blue (Fig. 4B). From the maximum amplitudes (blue arrows) and the difference absorption coefficients (Section 3.2.1), the cytochrome concentrations in the measuring cuvette can be calculated. These concentrations were divided by the total Chl concentration in the cuvette providing molar cyt/Chl ratios summarized in Fig. 4C. The numbers for the PSII and cyt $b_6 f$ complex content agree with published numbers [53]. For the cyt $b_6 f$ complex concentration, the average of the cyt f/Chl and the (cyt $b_6/2$)/Chl was used and for the total PSII amount in thylakoid membranes, the sum of cyt $b_{559}(HP)$ and cyt $b_{559}(LP)$. The statistical analysis reveals that the thylakoid membranes contain \sim 2.7 PSII complexes per cyt $b_6 f$ complex (Fig. 4C).

3.2.3. Quantification of cyt $b_6 f$ complex by heme staining of cyt f

The hemes in cytochromes of thylakoid membranes are usually noncovalently attached to their apoproteins. Rare exceptions are the heme of cyt f (c-type heme, f for frons (lat.) = leaf) that is covalently bound to the cyt f apoprotein [54] and the heme c_n bound to the cyt b_6 subunit [44,55,56]. The covalent heme-binding of c-type cytochromes leads to quantitative retention of their hemes during SDS-PAGE [57]. This facilitates the quantification of cvt $b_6 f$ from the cvt f content in a denaturating SDS-PAGE gel, i.e. under conditions in which all non-covalently bound hemes are washed away. Fig. 5A shows an example of Coomassie stained SDS-PAGE gel of two thylakoid membrane preparations. The corresponding TMBZ-based heme staining of the same gel in Fig. 5B confirms that only the cyt f (molecular weight 33 kDa) is visible on the gel. For reasons that are unclear the covalently-bound heme c_n of the cyt b₆ subunit (~24 kDa) is usually not visible or seen as a faint band in our gels. For the quantification of the cyt f heme signal, isolated cyt c standard samples from equine heart in two different quantities were run in parallel on the same gel (Fig. 5B, right). We checked that the two cyt c concentrations fall into the linear signal intensity range (Fig. 5C, two data points in the middle). The two cyt c reference bands were used to quantify the cyt f content by comparison of band intensities. The statistical analysis (Fig. 5D) gives 0.94 mmol cyt f per mol Chl. This biochemically-derived value is very close to the 1.00 mmol cvt $b_6 f$ complex per mol Chl derived from difference absorption spectroscopy (previous section).

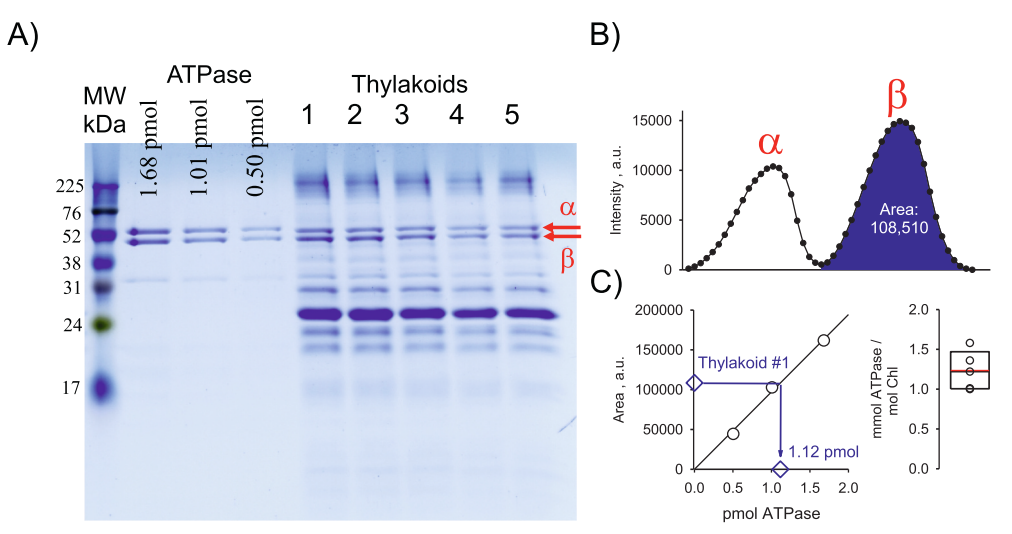


Fig. 7. SDS PAGE-based quantification of the ATP synthase β-subunit in thylakoid membranes, A. Example of an SDS PAGE with isolated ATPase standards in different amounts (left) and five different thylakoid samples (right). The positions of the ATPase α - and β -bands are indicated by red arrows. B, Intensity profiles of the α - and β -bands, showing good separation of the two bands. The area for the β -band is shaded in blue. C, Calibration curve for the \(\theta\)-subunit deduced from the isolated ATPase protein standards (panel A, left). An example for quantification of the β -subunit from the area under the gel band (see B) is shown by blue arrows. Right, Statistics of ATPase quantification of membranes by method.

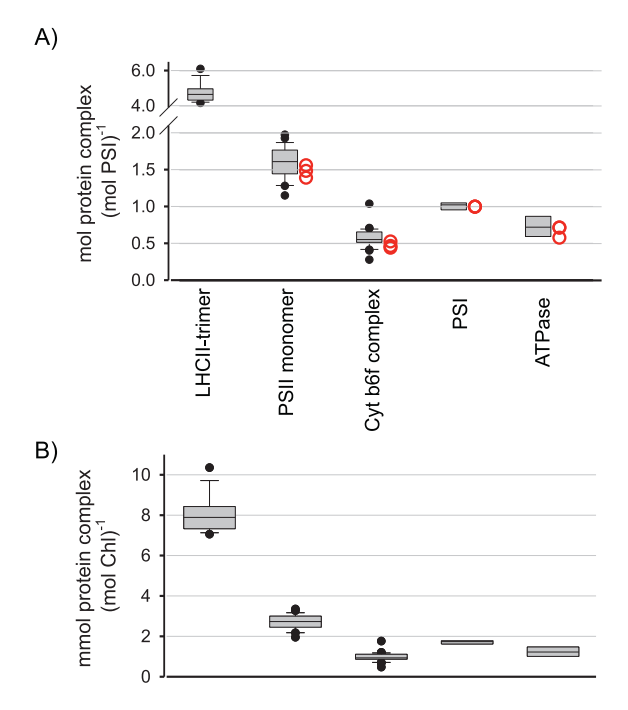


Fig. 8. Summary of the quantification of the main protein complexes in thylakoid membranes. A, Content of the protein complexes as normalized to PSI. For LHCII and cyt $b_6 f$ complex abundance, values from the two independent methods were averaged. Red circles show protein complex stoichiometries as obtained by the MS method. B, Protein contents normalized to Chl. MS-derived stoichiometries are riBAQ-based recalculations of an earlier published data set [29].

3.3. Quantification of PSI

The reaction center chlorophyll of PSI, P700, is a good candidate for the quantification of this protein complex since it has a well-established one-to-one stoichiometry with PSI and has a very specific difference absorption spectrum characterized by a strong bleaching of the absorption signal at 702 nm caused by the oxidized P700 species (P700⁺) [21]. A quantitative reduced to oxidized redox change of P700, as induced by a strong light pulse, in detergent-solubilized thylakoid membranes is shown in Fig. 6A. For this measurement, the electron donor sodium ascorbate was added. Electron flow from PSI was facilitated by the addition of the electron acceptor methylviologen. We further tested whether the light induced absorption change under our conditions reflects solely of P700 redox changes by comparing its wavelength dependency with a published P700⁺ minus P700 spectrum of isolated PSI [21]. The congruence between both spectra in Fig. 6B confirms that the signal in Fig. 6A reflects the reduced to oxidized change of P700 only. From the difference spectroscopic analysis, a ratio of 1.7 mmol PSI per mol of Chl was deduced (Fig. 6C), which is in line with published numbers for Arabidopsis PSI [29,58].

3.4. Quantification of ATP synthase

In contrast to respiratory membranes, which contain mostly dimeric ATP synthase complexes, the ATPase in thylakoid membranes occurs as monomers [59]. The quantification of the ATP synthase is probably the most challenging one among the main thylakoid protein complexes since it is redox inactive and contains no pigments. For this reason, quantitative SDS-PAGE gel electrophoresis is a viable approach [20,60]. The α -and β -subunits of the CF1 part of the ATP synthase represent good markers for quantitative SDS PAGE analysis of thylakoid membranes because no other protein subunits migrate in this molecular weight region (Fig. 7A). To this end, a protein gel-based approach similar to that

used for LHC II was employed (Fig. 2). In detail, thylakoid samples were run together with a known amount of isolated ATPase complex on the same gel (Fig. 7A). From the band intensity profile of the β -subunit, the area under the profile was deduced (Fig. 7B). The dilution curve of the ATP synthase standard in Fig. 7C verifies the linearity of the stain intensity. From the regression line of the isolated ATPase protein standard, the pmol ATPase of the thylakoid sample can be calculated and normalized to the Chl amount (Fig. 7C, right). An ATP synthase concentration of \sim 1.2 mmol/mol Chl agrees with published data [61].

3.5. MS-based relative quantification of thylakoid protein complexes

With the latest advancement in ionization and detection technologies, label-free shotgun LC-MS-MS has become a powerful tool for quantification of the entire proteome. Calculation using normalized precursor ion intensity in the form of the riBAQ method allows quantification over a wider dynamic range and removes bias against low abundant proteins. Results from the label-free mass spectrometric quantification of thylakoid protein complexes are presented as ratios to PSI in Fig. 8A. The ratios are in good agreement with those derived from spectroscopic and quantitative gel electrophoresis methods. For quantification of multiunit complexes, the MS-based label-free method has turned out to be especially robust as it benefits from the averaging of riBAQ values of multiple subunits of each complex. The label-free and the more versatile metabolic labeling methods of quantitative mass spectrometry have been widely used for the comparative analysis (as ratios) of photosynthetic proteomes under different treatments and genetic backgrounds. However, these methods do not give the absolute abundance or concentration of thylakoid protein complexes or individual proteins per total protein or chlorophyll. The development of stable isotope-labeled synthetic peptide standards makes absolute quantification now possible for thylakoid proteins.

3.6. Conclusions

In this study, a complementary set of biophysical and biochemical methods including mass spectrometry is presented that allows quantification of the protein complexes of thylakoid membranes. These methods are not only applicable for isolated entire thylakoid membranes but also thylakoid subfractions (e.g. stacked or unstacked thylakoid domains), chloroplasts, protoplasts, or even leaves if crude thylakoid extraction protocols are available. Furthermore, the methods presented here can be used for other species including gymnosperms and algae as long as a thylakoid isolation protocol is available. Isolated thylakoid membranes are required for all gel electrophoresis-based quantifications since interference by non-thylakoid proteins with similar molecular weights will lead to incorrect quantifications. For LHCII and cyt $b_0 f$ complex quantifications new methods are presented, which give numbers for the protein concentration that agree well with numbers derived using other published protocols.

Fig. 8 summarizes the protein concentrations of thylakoid membranes by combining all methods. The upper panel of Fig. 8 shows the protein complex abundances in Arabidopsis thylakoid membranes relative to PSI as derived from both quantitative spectroscopic and MS methods. As reported earlier (e.g. [19,53,61]), the relative stoichiometries are far from equal. An interesting observation is that the cyt $b_6 f$ complex, which carries out the rate limiting reaction of the photosynthetic electron transport chain, is the least abundant protein complex (~57 % relative to PSI and ~36 % to PSII). The sub-stoichiometric amount of the cyt $b_6 f$ complex relative to the two photosystems ensures strong control of steady-state electron transport by this complex using regulatory processes like photosynthetic control [6]. For example, if cyt $b_6 f$ complex to PSII ratio would instead be larger, then the control capability of cyt b₆f complex on electron transport would be lowered because of an increase in the rate limiting enzyme (see 'control theory', [62]).

Table 1Estimated total Chl distribution to PSII and PSI for different percentages of LHCII attached to PSI. The %LHCII bound to PSI giving an almost even distribution of Chls to both photosystems is shaded grey. For further details see in the text.

Protein	Chl per complex	Ratio rel. to PSI	Antenna sizes (# Chls) for different %LHCII bound to PSI			
			20%	30%	35%	40%
LHCII ₃	42	4.8				
PSII+CP24+CP26+CP29	74					
85% PSII active		1.4	265	245	235	225
100% PSII active		1.6	280	260	249	239
PSI-LHCI ₄	160	1	200	220	231	241

Table 2
Calculated protein membrane densities based on the measured molar protein to Chl ratios. For the conversion of the molar ratio to particle densities, a thylakoid area per Chl ratio of 1.71 nm² was used [20].

Protein	mmol / (mol Chl)	Particles μm ⁻² thylakoid	Particles μm ⁻² monomer (m) or dimer (d)	Particles μm ⁻² stacked (s) or unstacked (u)	Lit.	Measured/Literature
LHCII ₃	8.09	4733	4733 (m)	6176 (s) ^a	6257 ^c	1.0
PSII	2.70	1581	790 (d)	1185 (s)	1131 ^{d,e}	1.0
Cyt $b_6 f$	0.97	567	284 (d)	284 (s + u)	262^{f}	1.1
PSI	1.70	993	993 (m)	2980 (u) ^b	2450 ^e	1.0
ATPase	1.23	722	722 (m)	2165 (u)	1711 ^{d,g}	1.3

- a Assuming that 87 % of LHCII₃ is in stacked and 13 % in unstacked thylakoid regions (unpublished results). This is in line with other ultrastructural data [64].
- b Assuming that 18 % of PSI is in stacked and 82 % in unstacked thylakoid regions (unpublished results). This is in line with other ultrastructural data [64].
- ^c Freeze-fracture barley chloroplasts with rotary-shadowing [65].
- ^d Cryo-electron tomography on *Chlamydomonas* cells [66].
- e Atomic force microscopy on isolated stacked and unstacked thylakoid membranes from spinach [13].
- f Atomic force microscopy on isolated stacked thylakoid membranes from spinach [67].
- ^g Cryo-electron tomography on pea and spinach chloroplasts [59].

Another intriguing stoichiometric mismatch is between both photosystems with PSII being ~1.6 times more abundant than PSI. Although the PSII/PSI ratio changes under different environmental conditions (e. g. light quality or intensity [16,19]), the question arises as to how the light harvesting is balanced between the two photosystems in particular under low light intensities when the efficiency of photosynthetic light energy conversion should be maintained high. In this respect, the distribution of LHCII to both photosystems is crucial. Evidence exists that up to 15 % of PSII in thylakoid membranes is functionally inactive, i.e. that they are unable to reduce the secondary quinone acceptor Q_B (reviewed in [63]). Based on our PSII/PSI ratio, it follows that the PSII (active)/PSI ratio can drop from 1.6 to ~1.4 if inactive centers are considered. To estimate the fraction of LHCII connected to PSI in Table 1, we assumed that either all (100 %) or 85 % of PSII are active. It follows that 35 to 40 % of the major LHCII pool must be functionally attached to PSI, with the rest to PSII, to establish an equal Chl distribution between both photosystems (Table 1). These numbers might in fact be a bit lower since the energy conversion efficiency of PSII is lower $(\sim 85 \%)$ than that of PSI $(\sim 100 \%)$, i.e. 30 to 34 % of LHCII should be attached to PSI. The prediction that $\sim 1/3$ of the total LHCII pool is attached to PSI is in line with the recent postulate that a significant fraction of LHCII trimers is attached to PSI probably in the margins of grana thylakoids (reviewed in [32]). Furthermore, knowledge of the molar protein complex to Chl ratio (lower panel in Fig. 8) allows estimation of the protein densities in thylakoid membranes (# particles per μ m²) using a few assumptions (see legend to Table 2). The conversion of protein concentration to particle densities in thylakoid membranes (Table 2) reveals a good agreement with published protein density data derived from electron microscopic studies (column "Measured/ Literature").

Declaration of competing interest

Helmut Kirchhoff reports financial support was provided by US Department of Energy and the National Science Foundation USA.

Data availability

Data will be made available on request.

Acknowledgments

This work was supported by the National Science Foundation (MCB-BSF-1953570) and the Department of Energy (DE-SC0017160) to H.K. and Department of Energy (DE-SC0020639) to S.P. The authors thank Dr. Georg Groth (University of Düsseldorf, Germany) for the very kind gift of isolated ATPase.

References

- B.M. Slepchenko, J.C. Schaff, I. Macara, L.M. Loew, Quantitative cell biology with the virtual cell, Trends Cell Biol. 13 (2003) 570–576.
- [2] R. Mogilner, W.F.Marshall Wollman, Quantitative modeling in cell biology: what is it good for? DevelopmCell 11 (2006) 279–287.
- [3] J. Zaks, K. Amarnath, D.M. Kramer, K.K. Niyogi, G.R. Fleming, A kinetic model of rapidly reversible nonphotochemical quenching, Proc. Natl. Acad. Sci. U. S. A. 109 (2012) 15757–15762.
- [4] F.W. Moejes, et al., A systems-wide understanding of photosynthetic acclimation in algae and higher plants, J. Exp. Bot. 68 (2017) 2667–2681.
- [5] M. Li, V. Svoboda, G. Davis, D. Kramer, H.H. Kunz, H. Kirchhoff, Impact of ion fluxes across thylakoid membranes on photosynthetic electron transport and photoprotection. Nat. Plants 7 (2021) 979–988.
- [6] J.E. Johnson, J.A. Berry, The role of cytochrome b6f in the the control of steady state photosynthesis: a conceptual and quantitative model, Photosyn. Res. 148 (2021) 101–136.
- [7] A.R. Schneider, P.L. Geissler, Coexistence of fluid and crystalline phases of proteins in photosynthetic membranes, Biophys. J. 105 (2013) 1161–1170.
- [8] W.H.J. Wood, M.P. Johnson, Modeling the role of LHCII-LHCI, PSII-LHCII, and PSI-LHCII interactions in state transitions, Biophys. J. 119 (2020) 287–299.
- [9] R. Höhner, M. Pribil, M. Herbstova, L.S. Lopez, H.H. Kunz, M. Li, M. Wood, M. Svoboda, S. Puthiyaveetil, D. Leister, H. Kirchhoff, Plastocyanin is the long-range electron carrier between photosystem II and photosystem I in plants, Proc. Natl. Acad. Sci. USA 117 (2020) 15354–15362.
- [10] N. Liguori, R. Croce, S.J. Marrink, S. Thallmair, Molecular dynamics simulations in photosynthesis, Photosyn. Res. 144 (2020) 273–295.
- [11] P.-A. Albertsson, A quantitative model of the domain structure of the photosynthetic membrane, Trends Plant Sci. 6 (2001) 349–354.

- [12] J.P. Dekker, E.J. Boekema, Supramolecular organization of thylakoid membrane proteins in green plants, Biochim. Biophys. Acta 1706 (2005) 12–39.
- [13] W.H.J. Wood, C. MacGregor-Chatwin, S.F.H. Barnett, G.E. Mayneord, X. Huang, J. K. Hobbs, C.N. Hunter, M.P. Johnson, Dynamic thylakoid stacking regulates the balance between linear and cyclic photosynthetic electron transfer, Nat. Plants 4 (2018) 116–127.
- [14] D. Govindjee, L.O.Björn Shevela, Evolution of the Z-scheme of photosynthesis, Photosyn. Res. 131 (2017) 351–359.
- [15] J.M. Anderson, Photoregulation of the composition, function, and structure of thylakoid membranes, Ann. Rev. Plant Physiol. 37 (1986) 93–136.
- [16] W.S. Chow, A. Melis, J.M. Anderson, Adjustments of photosystem stoichiometry in chloroplasts improve the quantum efficiency of photosynthesis, Proc. Natl. Acad. Sci. U. S. A. 87 (1990) 7502–7506.
- [17] I.M. Ibrahim, S.D. McKenzie, J. Chung, U.K. Aryal, W.D. Leon-Salas, S. Puthiyaveetil, Photosystem stoichiometry adjustment is a photoreceptormediated process in arabidopsis, Sci. Rep. 12 (2022) 10982.
- [18] S.E. Flannery, F. Pastorelli, W.H.J. Wood, C.N. Hunter, M.J. Dickman, P.J. Jackson, M.P. Johnson, Comparative proteomics of thylakoids from Arabidopsis grown in laboratory and field conditions, Plant Direct 5 (2021), e355.
- [19] J.M. Anderson, W.S. Chow, D.J. Goodchild, Thylakoid membrane organisation in sun/shade acclimation, Aust. J. Plant Physiol. 15 (1988) 11–26.
- [20] H. Kirchhoff, U. Mukherjee, H.J. Galla, The molecular architecture of the thylakoid membrane: the lipidic diffusion space for plastoquinone, Biochemist 41 (2002) 4872, 4882.
- [21] B. Ke, The rise time of photoreduction, difference spectrum, and oxidation-reduction potential of P430, Arch. Biochem. Biophys. 152 (1972) 70–77.
- [22] R.J. Porra, W.A. Thompson, P.E. Kriedermann, Determination of accurate extinction coefficient and simultaneous equations for essaying chlorophylls a and b extracted with four different solvents: verification of the concentration of chlorophyll standards by atomic absorption spectroscopy, Biochim. Biophys. Acta 975 (1989) 384–394.
- [23] R. Fristedt, A. Herdean, C.E. Blaby-Haas, F. Mamedov, S.S. Merchant, R.L. Last, B. Lundin, PHOTOSYSTEM II PROTEIN33, a protein conserved in the plastid lineage, is associated with the chloroplast thylakoid membrane and provides stability to photosystem II supercomplexes in arabidopsis, Plant Physiol. 167 (2015) 481–492.
- [24] H. Schagger, Tricine-SDS-PAGE, Nat. Protoc. 1 (2006) 16-22.
- [25] H. Koochak, S. Puthiyaveetil, D.L. Mullendore, M. Li, H. Kirchhoff, The structural and functional domains of plant thylakoid membranes, Plant J. 97 (2019) 412–429.
- [26] H. Kirchhoff, H.-J. Hinz, J. Rösgen, Aggregation and fluorescence quenching of chlorophyll a of the light-harvesting complex II from spinach in vitro, Biochim. Biophys. Acta 1606 (2003) 105–116.
- [27] U.K. Laemmli, Cleavage of structural proteins during the assembly of the head of bacteriophage T4, Nature 227 (1970) 680–685.
- [28] A. Färber, A.J. Young, A.V. Ruban, P. Horton, P. Jahns, Dynamics of xanthophyll-cycle activity in different antenna subcomplexes in the photosynthetic membranes of higher plants: the relationship between zeaxanthin conversion and nonphotochemical fluorescence quenching, Plant Physiol. 115 (1997) 1609–1618.
- [29] S.D. McKenzie, I.M. Ibrahim, U.K. Aryal, S. Puthiyaveetil, Stoichiometry of protein complexes in plant photosynthetic membranes, Biochim. Biophys. Acta 1861 (2020), 148141.
- [30] K.J. Spinelli, et al., Distinct energy metabolism of auditory and vestibular sensory epithelia revealed by quantitative mass spectrometry using MS2 intensity, Proc. Natl. Acad. Sci. U. S. A. 109 (2012) 268–277.
- [31] S. Jansson, A guide to the lhc genes and their relatives in Arabidopsis, Trends Plant Sci. 4 (1999) 1360–1385.
- [32] M. Rantala, S. Rantala, E.-M. Aro, Composition, phosphorylation, and dynamic organization of photosynthetic protein complexes in plant thylakoid membranes, Photochem. Photobiol. Sci. 19 (2020) 604–619.
- [33] P. Cao, X. Su, X. Oan, Z. Liu, W. Chang, M. Li, Structure, assembly and energy transfer of plant photosystem II supercomplex, Biochim. Biophys. Acta 1859 (2018) 633–644.
- [34] H. Kirchhoff, W. Haase, S. Wegner, R. Danielsson, R. Ackermann, P.-A. Albertsson, Low-light-induced formation of semicrystalline photosystem II arrays in higher plant chloroplasts, Biochemist 46 (2007) 11169–11176.
- [35] R. Kouril, E. Wientjes, J.B. Bultema, R. Croce, E.J. Boekema, High-light vs. Low-light: effect of light acclimation on photosystem II composition and organization in Arabidopsis thaliana, Biochim. Biophys. Acta 1827 (2013) 411–419.
- [36] P. Dainese, R. Bassi, Subunit stoichiometry of the chloroplast photosystem II antenna system and aggregation state of the component chlorophyll a/b binding proteins, J. Bio. Chem. 266 (1991) 8136–8142.
- [37] S. Caffarri, R. Kourik, S. Kereiche, E.J. Boekema, R. Croce, Functional architecture of higher plant photosystem II supercomplexes, EMBO J. 28 (2009) 3052–3963.
- [38] Z. Huang, L. Shen, W. Wang, Z. Mao, X. Yi, T. Kuang, J.-R. Shen, X. Zhang, G. Han, Structure of photosystem I-LHCI-LHCII from the green alga Chlamydomonas reinhardtii in state 2, Nat. Commun. 12 (2021) 1100.

- [39] X. Qin, M. Suga, T.Y. Kuang, S.R. Shen, Crystal structure of plant photosystem I-LHCI super-complex at 2.8 angstrom resolution, Science 348 (2015) 989–995.
- [40] P. Müller-Moule, P.L. Conklin, K.K. Niyogi, Ascorbate deficiency can limit violaxanthin de-expoxidase activity in vivo, Plant Physiol. 128 (2002) 970–977.
- [41] W.A. Cramer, J. Whitmarsh, Photosynthetic cytochromes, Ann. RevPlant Physiol. 28 (1977) 133–172.
- [42] S.U. Metzger, W.A. Cramer, J. Whitmarsh, Critical analysis of the extinction coefficient of chloroplast cytochrome f, Biochim. Biophys. Acta 1319 (1997) 233–241.
- [43] D.H. Steward, G.W. Brudvig, Cytochrome b559 of photosystem II, Biochim. Biophys. Acta 1367 (1998) 63–87.
- [44] L.A. Malone, et al., Cryo-EM structure of the spinach cytochrome b6f complex at 3.6 Å resolution, Nature 575 (2019) 535–539.
- [45] D. Baniulis, E. Yamashita, H. Zhang, S.S. Hasan, W.A. Cramer, Structure-function of the cytochrome b6f complex, Photochem. Photobiol. 84 (2008) 1349–1358.
- [46] L.A. Malone, M.S. Proctor, A. Hitchcock, C.N. Hunter, M.P. Johnson, Cytochrome b6f – orchestrator of photosynthetic electron transfer, Biochim. Biophys. Acta 1862 (2021), 148380.
- [47] W.S. Chow, A.B. Hope, The stoichiometries of supramolecular complexes in thylakoid membranes from spinach chloroplasts, Aust. J. Plant Physiol. 14 (1987) 21–28.
- [48] C.A. Buser, B.A. Diner, G.W. Brudvig, Reevaluation of the stoichiometry of cytochrome b559 in photosystem II and thylakoid membranes, Biochemist 31 (1992) 11441–11448.
- [49] R. Danielsson, P.-A. Albertsson, F. Mamedov, S. Styring, Quantification of photosystem I and II in different parts of the thylakoid membrane from spinach, Biochim. Biophys. Acta 1608 (2004) 53–61.
- [50] S.W. McCauley, A. Melis, Quantification of photosystem II in spinach thylakoids, Biochim. Biophys. Acta 849 (1986) 175–182.
- [51] J.M. Anderson, A. Melis, Localization of different photosystems in separate regions of chloroplast membranes, Proc. Natl. Acad. Sci. U. S. A. 80 (1983) 745–749.
- [52] R. Danielsson, M. Suorsa, V. Paakarinen, P.-A. Albertsson, S. Styring, E.-M. Aro, F. Mamedov, Dimeric and monomeric organization of photosystem II, J. Biol. Chem. 281 (2006) 14241–14249.
- [53] M.A. Schöttler, S.Z. Toth, Photosynthetic complex stoichiometry dynamics in higher plants: environmental acclimation and photosynthetic flux control, Front. Plant Sci. 5 (2014) 188.
- [54] W.A. Cramer, S.E. Martinez, D. Huang, G.S. Tae, R.M. Everly, J.B. Heymann, R. H. Cheng, T.S. Baker, J.L. Smith, Structural aspects of the cytochrome b6f complex; structure of the lumen-side domain of cytochrome f, J. Bioenerg. Biomembr. 26 (1994) 31–47.
- [55] G. Kurisu, H. Zhang, J.L. Smith, W.A. Cramer, Structure of the cytochrome b6f complex of oxygenic photosynthesis: tuning the cavity, Science 302 (2003) 1009–1014.
- [56] D. Stroebel, Y. Choquet, J.L. Popot, D. Picot, An atypical haem in the cytochrome b (6)f complex, Nature 426 (2003) 413–418.
- [57] C.F. Goodhew, K.R. Brown, G.W. Pettigrew, Haem staining in gels, a useful tool in the study of bacterial c-type cytochromes, Biochim. Biophys. Acta 852 (1986) 288–294.
- [58] S. Puthiyaveetil, T. Woodiwiss, R. Knoerdel, A. Zia, M. Wood, R. Hoehner, H. Kirchhoff, Significance of the photosystem II core phosphatase PBCP for plant viability and protein repair in thylakoid membranes, Plant Cell Physiol. 55 (2014) 1245–1254.
- [59] B. Daum, D. Nicastro, J. Austin 2nd, J.R. McIntosh, W. Kühlbrandt, Arrangement of photosystem II and ATP synthase in chloroplast membranes of spinach and pea, Plant Cell 22 (2010) 1299–1312.
- [60] H.R. Fiedler, S. Ponomarenko, N. von Gehlen, H. Strotmann, Proton gradientinduced changes of the interaction between CF0 and CF1 as probed by cleavage with NaSCN, Biochim. Biophys. Acta 1188 (1994) 29–34.
- [61] M. Pribil, M. Labs, D. Leister, Structure and dynamics of thylakoids in land plants, J. Exp. Bot. 65 (2014) 1955–1972.
- [62] H. Kacser, J.A. Burns, Molecular democracy: who shares the controls? Biochem. Soc. Trans. 7 (1979) 1149–1160.
- [63] J. Lavergne, J.M. Briantais, Photosystem II heterogeneity, in: D.R. Ort, C.F. Yocum (Eds.), Oxygenic Photosynthesis: The Light Reactions, Springer Press, 1996, pp. 265–287.
- [64] L.A. Staehelin, Chloroplast structure and supramolecular organization of photosynthetic membranes, in: L.A. Staehelin, C.J. Arntzen (Eds.), Photosynthesis III: Photosynthetic Membranes and Light-harvesting Systems, Springer-Verlag, Berlin, 1986, pp. 1–84.
- [65] D. Simpson, Freeze-fracture studies of mutant barley chloroplast membrane, in: L. A. Staehelin, C.J. Arntzen (Eds.), Photosynthesis III, Springer, 1986, pp. 665–674.
- [66] W. Wietrzynski, M. Schaffer, D. Tegunov, S. Albert, A. Kanazawa, J.M. Plitzko, W. Baumeister, B.D. Engel, Charting the native architecture of chlamydomonas thylakoid membranes with single-molecule precision, eLife 9 (2020), e53740.
- [67] M.P. Johnson, C. Vasilev, J.D. Olson, C.N. Hunter, Nanodomains of cytochrome b6f and photosystem II complexes in spinach grana thylakoid membranes, Plant Cell 26 (2014) 3051–3061.